Isotropy Study for Over-the-Air Measurements in a Loaded Reverberation Chamber*

Damir Senic, Diego Cavaliere, Matt V. North, Maria G. Becker, Kate A. Remley,
Chih-Ming Wang, Christopher L. Holloway
National Institute of Standards and Technology
Boulder, CO
damir.senic@nist.gov

***Abstract*—We performed a field isotropy study based on the reverberation chamber transfer function for three different reverberation chamber configurations. Guidance for reducing the anisotropy based on the polarization-balanced antenna is also provided. We show that chamber isotropy is strongly influenced by loading such that an unloaded chamber can be considered as an isotropic environment, while a loaded chamber is more-or-less anisotropic depending on the amount of loading present. The loading of the chamber is crucial for wireless tests involving modulated signals. Its purpose is to create a flat channel, which enables successful demodulation of the signal without distortion. Consequently, understanding this effect is important in quantifying measurement uncertainty in loaded conditions.**

Keywords—dipole antenna; isotropy; loading; polarization balance; reverberation chamber; wireless tests

I. Introduction

Reverberation chambers can be considered to be electrically-large resonators where, ideally, fields impinge on the device under test (DUT) equally from all directions creating rich isotropic environments [1],[2]. Many metrics, including the chamber transfer function [2],[3], antenna efficiency [4]-[7], shielding effectiveness [8],[9], absorption cross section [10]-[14], spatial correlation [15],[16], *etc*. have been derived under an isotropy premise. However, direct evaluation and confirmation of chambers' isotropy have been lacking. To the authors' knowledge, studies that investigated isotropy inside reverberation chambers are limited to a select few [2],[17],[18].

Empirical study of real reverberation chamber isotropy is particularly interesting to the wireless community, which employs reverberation chambers for over-the-air (OTA) tests [2],[19]-[22]. Contrary to electromagnetic compatibility (EMC) tests, wireless tests of modulated signals generally require a loaded chamber. Loading broadens and flattens the channel inside the chamber, which is necessary for demodulating modulated signals without distortion [3],[23]. However, heavy loading also has negative impacts on the chamber's behavior, as it decreases field homogeneity and increases chamber anisotropy primarily due to the unstirred multipath components. Hence, real-world deviations from ideal chamber isotropy will affect basic metrics unless compensated for by the stirring sequence.

A real reverberation chamber setup will exhibit some anisotropy depending on the amount of loading. The level of anisotropy is an important figure of merit in standardized tests. A common way to characterize the chamber isotropy is based on polarization balance, where the electric field or received power is measured for each of three orthogonal orientations of a field probe or an antenna. This method for performing isotropy characterization of a reverberation chamber is described in the IEC 61000-4-21 standard [24]. The IEC test proposes electric-field measurements with an electric-field probe capable of measuring three orthogonal polarizations at eight different locations inside the chamber that form the edge of the chamber's working volume. Electric-field probes are suggested because they have small dimensions and should, therefore, not perturb the fields inside the chamber. The small size of the field probe also means that undesirable field averaging characteristic of larger antennas can be avoided. Tuned dipoles are sometimes used for this purpose, as well.

In this paper, the assumption of a statistically isotropic reverberation chamber environment is evaluated by measuring the transfer function for different dipole antenna orientations and loading cases at ten locations inside the chamber (see Fig. 1).

This paper is organized as follows: the measurement setup and procedures for measuring polarization balance are given in Section II. Section III follows with the isotropy measurement results and evaluation of a chamber in terms of measured anisotropy. In Section IV, guidance for reducing the chamber's anisotropy is given. Statistical analysis is given in Section V, and concluding remarks can be found in Section VI.

II. Chamber Setup for Polarization Balance Measurements

Polarization balance measurements were performed in terms of the chamber transfer function (G_{ref}) of a 1.9 m (l) × 1.4 m (w) × 2 m (h) reverberation chamber shown in Fig. 1. The chamber's transfer function (G_{ref}) is defined as

$$G_{\text{ref}} = \frac{\left\langle |S_{21}|^2 \right\rangle}{\eta_{\text{TX}}\eta_{\text{RX}}\left(1-\left|\langle S_{11}\rangle\right|^2\right)\left(1-\left|\langle S_{22}\rangle\right|^2\right)}, \quad (1)$$

where the brackets denote the ensemble average over the mode-stirring sequence, S_{21} is the forward transmission scattering parameter measured by a VNA, and the terms in the

* Work supported by U.S. government, not protected by U.S. copyright

denominator represent the free-space radiation efficiencies (η_{TX} and η_{RX}) and mismatch corrections for the two antennas. The radiation efficiency can be measured in either an anechoic chamber or in an unloaded reverberation chamber [4]-[7]. The chamber was equipped with a pair of electrically large paddles and a turntable. One paddle moved a maximum vertical distance of 1.4 m spanning the length of the chamber's side wall. The other paddle moved a maximum horizontal distance of 1.3 m spanning the length of the chamber's ceiling. The longitudinal resolution of both paddles was 7.5 μm. The angular resolution of the turntable was 0.005°, according to manufacturer's specifications. All measurements are made in stepped mode under stationary conditions.

Measurements were performed over the Personal Communications Service (PCS) band (1850 MHz – 1990 MHz) [22] with a linearly-polarized, half-wavelength dipole receive (RX) antenna oriented in the three orthogonal orientations mounted on the turntable. Horizontal and vertical translation stages, combined with the turntable, were used to automate positioning of the receive antenna (see Fig. 2) at the ten different locations shown in Fig. 1. The first four locations were on the edge of the lower base of the cylinder indicated in Fig. 1, separated by 90° of the turntable rotation. The fifth position was at the center of the cylinder's lower base. The other five locations were the same as the first five but elevated an additional 20 cm. At each RX antenna location, all *S*-parameters were measured for each of the three orthogonal polarizations.

Two different transmit antennas were used in this study. The first, shown in Fig. 3 (left), was a stationary, vertically polarized, broadband (650 MHz – 3.5 GHz) discone monopole antenna. It was used to quantify field anisotropy in Section III. The second, Fig. 3 (right), was a polarization-balanced, double-sided, tapered, self-grounded monopole antenna [25]. This antenna was used to demonstrate a method for reducing the effects of field anisotropy in Section IV. Measurements were performed with a 50 GHz VNA. Key measurement parameters are summarized in Table I. The transmit and receive antennas were physically separated by a metallic shield intended to avoid direct energy coupling between them (see Figs. 1 and 2).

In order to study the effect of chamber loading on isotropy, measurements were repeated for three different chamber loading configurations: unloaded, partially loaded, and heavily loaded. Loading was achieved with RF absorbers magnetically mounted on the chamber's walls, as shown in Fig. 2. For the heavily loaded case, five large absorbers with dimensions of 15 cm (l) × 6 cm (w) × 60 cm (h), and four small absorbers with dimensions of 15 cm (l) × 6 cm (w) × 15 cm (h), were used. Absorber layout and orientation for the heavily loaded chamber is shown in Figs. 1 and 2. The partially loaded chamber had three large absorbers. Chamber loading is commonly used to broaden the chamber's coherence bandwidth (CBW) and to create a flat channel in order to measure modulated signals. The CBWs corresponding to the unloaded, partially loaded, and heavily loaded chambers were 2.86 MHz, 7.76 MHz, and 12.26 MHz, respectively, calculated with the method of [23].

TABLE I. MEASUREMENT PARAMETERS

Parameter	Value
Frequency range	1850 MHz – 1990 MHz
Number of frequency points	1401
IF bandwidth	2 kHz
VNA output power level	-10 dBm
VNA dwell time	10 μs
Turntable locations (static)	10
Number of paddle positions-stepped ($V \times H$)	15 × 15

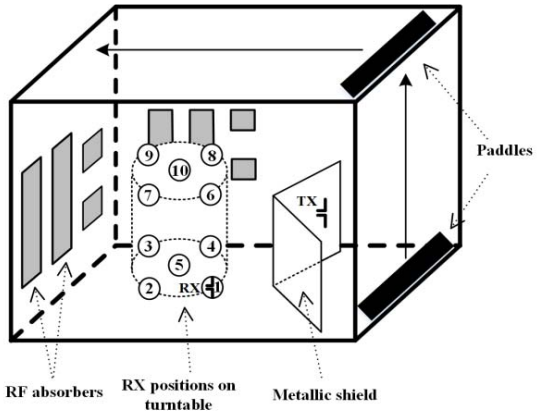

Fig. 1. Schematic of chamber setup for polarization balance measurements.

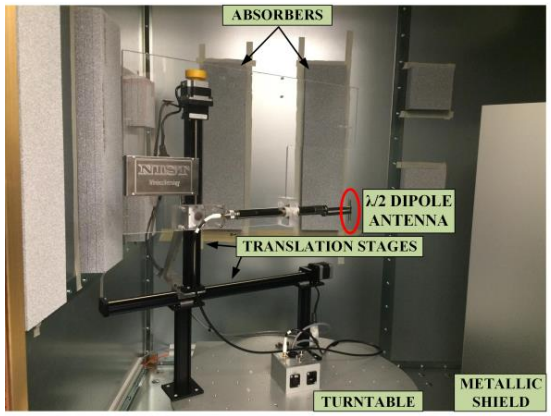

Fig. 2. Heavily loaded chamber and receive antenna fixture consisting of horizontal and vertical translation stages placed on the turntable.

Fig. 3. Two transmit antennas; left: vertically-polarized broadband discone monopole antenna; right: polarization-balanced, double-sided, tapered, self-grounded monopole antenna [25].

III. Evaluation of Reverberation Chamber Performance in Terms of Field Anisotropy

To study the effects of polarization imbalance as a function of loading, the method of [24] was used. The chamber transfer function (G_{ref}) from (1) was calculated for the three different chamber loading configurations and for ten RX antenna locations. The G_{ref} results, averaged over the PCS band, are summarized in Table II for the linearly-polarized TX antenna, at each RX antenna location and for each chamber loading configuration.

The unloaded chamber provides a nearly isotropic environment where the *Z* component is only 0.5 dB higher than the *X* and *Y* components. Regarding the partially loaded and heavily loaded chambers, differences of 0.22 – 1.43 dB and 0.88 – 5.23 dB, respectively, between the *Z* component and the *X* and *Y* components are observed. This effect is seen at each RX antenna location, as well as on average over the ten RX antenna locations shown at the bottom of Table II. Note that the dominance of the *Z* component is due to the vertical (*Z*) polarization of the TX antenna.

TABLE II. G_{REF} Results in Decibels for Vertically-Polarized Monopole TX Antenna Averaged over PCS Band

RX		RC	PARTLY	HEAVILY
Location	Orientation	UNLOADED	LOADED	LOADED
1	*X*	-18.07	-22.09	-27.14
	Y	-18.12	-22.32	-28.45
	Z	**-17.34**	**-21.08**	**-24.20**
2	*X*	-18.20	-22.25	-27.78
	Y	-17.93	-21.75	-27.35
	Z	**-17.87**	**-21.97**	**-25.67**
3	*X*	-18.03	-22.20	-27.65
	Y	-18.10	-22.34	-27.25
	Z	**-17.69**	**-20.99**	**-23.83**
4	*X*	-18.14	-22.13	-26.64
	Y	-18.10	-21.87	-26.31
	Z	**-17.77**	**-21.01**	**-23.39**
5	*X*	-17.97	-21.82	-28.36
	Y	-17.97	-22.00	-27.06
	Z	**-17.59**	**-20.82**	**-23.50**
6	*X*	-17.89	-21.81	-27.47
	Y	-18.02	-21.88	-25.00
	Z	**-17.30**	**-20.63**	**-22.24**
7	*X*	-18.25	-22.84	-25.54
	Y	-18.29	-22.39	-27.58
	Z	**-17.83**	**-21.55**	**-24.66**
8	*X*	-18.04	-22.19	-26.74
	Y	-18.04	-22.27	-25.07
	Z	**-17.25**	**-20.84**	**-24.02**
9	*X*	-18.07	-22.01	-24.13
	Y	-18.12	-21.78	-26.06
	Z	**-17.90**	**-21.30**	**-22.68**
10	*X*	-18.16	-22.21	-27.12
	Y	-18.05	-22.04	-26.50
	Z	**-17.48**	**-21.20**	**-24.22**
Average	*X*	-18.08	-22.15	-27.48
	Y	-18.07	-22.06	-27.26
	Z	**-17.60**	**-21.12**	**-24.53**

In Fig. 4 we show the measured G_{ref} averaged over the ten RX antenna locations (antenna stirring) for the vertically-polarized monopole TX antenna. Fig. 4 a) through c) illustrate the trend of increased anisotropy with increased loading. The unloaded chamber results, given in Fig. 4, indicate that all three field components have similar values, as expected. With the addition of loading, the *Z* component becomes increasingly larger than the *X* and *Y* components. Note that in Fig. 4 a) and b) a 0.5 dB per division scale is used and in c) the scale is 2 dB per division.

The data presented in the plots of Fig. 4 are the result of averaging G_{ref} over ten turntable locations. Therefore, we see that antenna location stirring by itself does not improve field isotropy; only field homogeneity (spatial uniformity) can be improved, leading to the need for polarization stirring [2],[17] or other techniques, as described in the next section. In the next section, guidance for reducing the anisotropy in the case of a loaded reverberation chamber is provided.

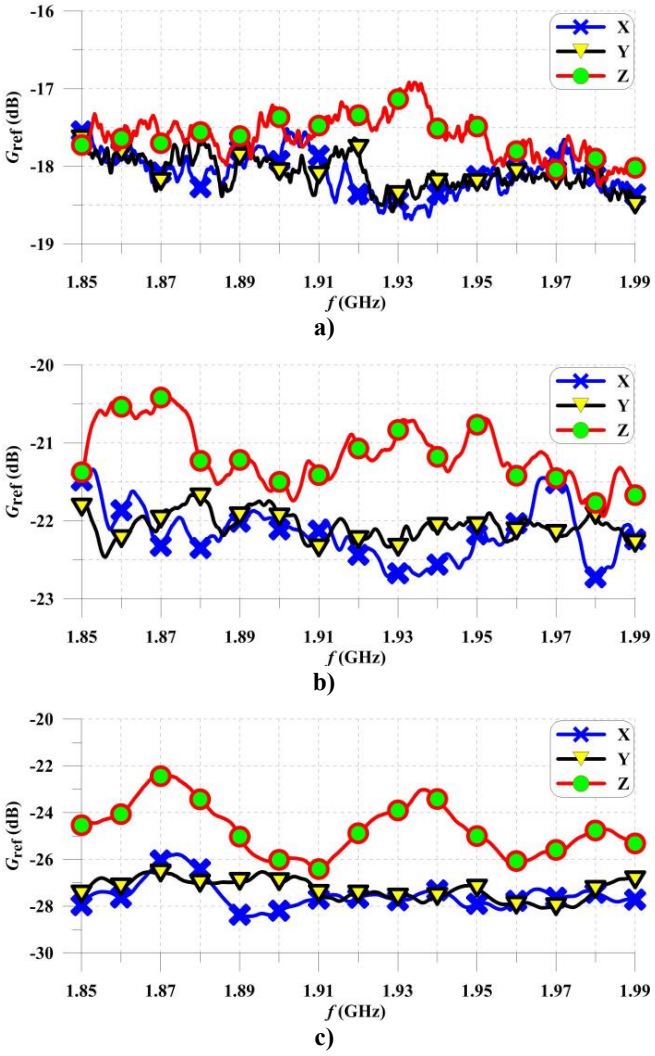

Fig. 4. G_{ref} measured over the PCS band and averaged over 10 RX antenna locations for a vertically-polarized monopole TX antenna inside: a) unloaded chamber, b) partially loaded chamber, and c) heavily loaded chamber.

IV. Methods for Reducing Reverberation Chamber Anisotropy

Many reverberation-chamber-based tests rely on linearly-polarized TX antennas such as monopole, dipole, log-periodic, loop, standard horn, and double-ridged horn antennas. As shown in the previous section, such antennas are capable of measuring isotropic environments as long as the chamber is not loaded. Hence, we can use linearly-polarized antennas for the majority of tests in EMC. However, since wireless tests generally require a loaded chamber, we should be aware of the effects of possible anisotropic chamber environments if linearly polarized antennas are used. Polarization stirring is one solution to this issue [2],[17].

In this section, we will show that besides polarization stirring, we can compensate for loading-induced field anisotropy by using a polarization-balanced antenna. Here, a double-sided, tapered, self-grounded monopole antenna [25], shown in Fig. 3 (right) was used in place of the linearly-polarized TX antenna. However, any kind of polarization-balanced antenna (such as a helix antenna in axial or end-fire mode) could be used for the same purpose.

TABLE III. G_{REF} Results in Decibels for Polarization-Balanced Monopole TX Antenna Averaged over PCS Band

RX		RC	PARTLY	HEAVILY
Location	**Orientation**	**UNLOADED**	**LOADED**	**LOADED**
1	***X***	-18.69	-22.53	-24.15
	Y	-18.81	-23.22	-24.72
	Z	**-18.58**	**-22.40**	**-23.53**
2	***X***	-18.97	-23.43	-25.46
	Y	-18.78	-22.50	-25.58
	Z	**-18.91**	**-23.08**	**-25.15**
3	***X***	-18.74	-22.67	-24.37
	Y	-18.81	-22.59	-24.73
	Z	**-18.70**	**-22.36**	**-23.83**
4	***X***	-18.81	-22.34	-23.91
	Y	-18.45	-21.16	-22.84
	Z	**-18.60**	**-21.78**	**-23.00**
5	***X***	-19.01	-22.86	-24.37
	Y	-18.79	-22.40	-23.75
	Z	**-18.72**	**-22.20**	**-23.57**
6	***X***	-18.58	-21.76	-23.92
	Y	-18.20	-22.17	-23.35
	Z	**-18.66**	**-22.44**	**-23.50**
7	***X***	-18.80	-23.24	-24.97
	Y	-18.70	-22.82	-24.64
	Z	**-18.66**	**-23.05**	**-24.77**
8	***X***	-18.76	-22.71	-23.67
	Y	-18.64	-22.26	-24.26
	Z	**-18.77**	**-22.47**	**-24.28**
9	***X***	-18.61	-22.39	-24.07
	Y	-18.35	-21.39	-22.52
	Z	**-18.56**	**-22.06**	**-23.14**
10	***X***	-18.89	-22.90	-24.93
	Y	-18.91	-22.48	-24.38
	Z	**-18.68**	**-22.30**	**-23.60**
Average	***X***	-18.79	-22.66	-24.35
	Y	-18.64	-22.26	-23.98
	Z	**-18.68**	**-22.40**	**-23.79**

In Table III, the chamber transfer function results for the polarization-balanced transmit antenna are shown for the ten RX antenna locations and three chamber loading configurations. Very similar G_{ref} values were measured for all three field components at all RX antenna locations and for all three chamber configurations. We conclude, therefore, that we can reduce the effects of field anisotropy due to the loading when a polarization-balanced antenna is used. This effect is shown in Fig. 5 a) through c), where the chamber transfer function is averaged over ten RX antenna locations. Similar G_{ref} results were obtained for all three field components for a partially loaded chamber (0.13 – 0.82 dB) and for heavily loaded chamber (0.02 – 1.33 dB).

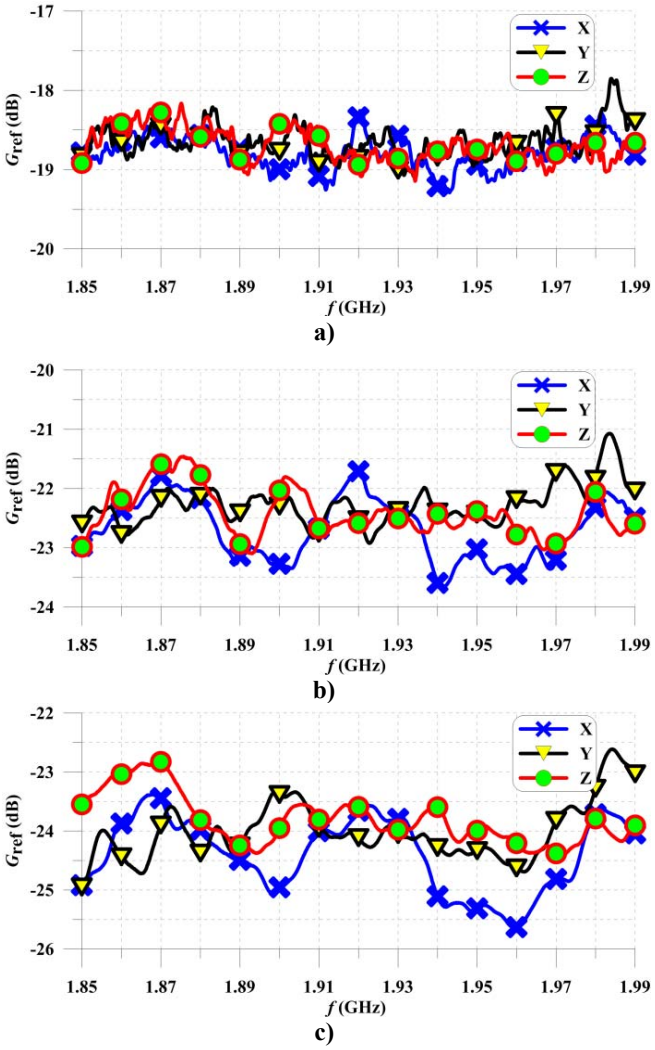

Fig. 5. G_{ref} measred over the PCS band and averaged over 10 RX antenna locations for a polarization-balanced monopole TX antenna inside: a) unloaded chamber, b) partially loaded chamber, and c) heavily loaded chamber.

V. STATISTICS

In order to evaluate the observed improvement in the average field isotropy when using a polarization-balanced antenna, we calculated the standard deviation of the G_{ref} values over the ten antenna locations for each chamber configuration and for each of the two different TX antennas. The results are given in Table IV where the standard deviations of the G_{ref} values for the unloaded chamber are shown to be similar for both TX antennas. Table IV shows that, as chamber loading increases, the standard deviation for the vertically-polarized monopole antenna becomes larger than the standard deviation for the polarization-balanced antenna. This is particularly true for the heavily loaded chamber, which indicates that care must be taken in choosing both stirring sequence and antennas to minimize the effect of field anisotropy due to loading.

TABLE IV. STANDARD DEVIATION OF G_{REF} IN DECIBELS FOR VERTICALLY-POLARIZED AND POLARIZATION-BALANCED MONOPOLE TX ANTENNAS

TX ANTENNA	RC UNLOADED	PARTLY LOADED	HEAVILY LOADED
Vertically-Polarized Monopole	**0.28**	**0.56**	**1.76**
Polarization-Balanced Monopole	**0.17**	**0.51**	**0.76**

We also characterized the chamber's performance in terms of field isotropy from the planar and total field anisotropy coefficients [24]

$$\left\langle A_{\alpha\beta} \right\rangle = \left\langle \frac{\left(\left|E_\alpha\right|^2 / P_{\text{i}}\right) - \left(\left|E_\beta\right|^2 / P_{\text{i}}\right)}{\left(\left|E_\alpha\right|^2 / P_{\text{i}}\right) + \left(\left|E_\beta\right|^2 / P_{\text{i}}\right)} \right\rangle = \left\langle \frac{\left|S_{21,\alpha}\right|^2 - \left|S_{21,\beta}\right|^2}{\left|S_{21,\alpha}\right|^2 + \left|S_{21,\beta}\right|^2} \right\rangle, \quad (2)$$

$$\left\langle A_{\text{total}} \right\rangle = \left\langle \sqrt{\left(A_{XY} + A_{XZ} + A_{YZ}\right)/3} \right\rangle, \quad (3)$$

where $|E_{\alpha,\beta}|$ and $S_{21,\alpha,\beta}$ represent the measured received field strength and forward transmission scattering parameter, respectively, of the arbitrary rectangular component α or $\beta = X$, Y, Z and P_{i} is the net input power injected into the chamber.

Anisotropy coefficients from [24] were calculated for the two different TX antennas and three chamber configurations given in Table V. According to the method of [24] (Annex J), we compared them with typical coefficient values for "medium" and "good" reverberation chamber quality, as shown in Table VI. Because we used $15 \times 15 = 225$ paddle positions, all calculated anisotropy coefficients fall either in the "good" or "medium" chamber quality category. Bearing in mind the observed polarization imbalance for the heavily loaded chamber excited by the vertically-polarized monopole antenna, we conclude that the current standard test method [24] is rather forgiving considering field anisotropy.

TABLE V. CALCULATED TOTAL FIELD ANISOTROPY COEFFICIENTS FOR THREE CHAMBER CONFIGURATIONS AND TWO TX ANTENNAS

TX ANTENNA	RC UNLOADED	PARTLY LOADED	HEAVILY LOADED
Vertically-Polarized Monopole	**-14.03**	**-11.28**	**-10.79**
Polarization-Balanced Monopole	**-17.68**	**-14.55**	**-13.60**

TABLE VI. TYPICAL VALUES FOR TOTAL FIELD ANISOTROPY COEFFICIENTS FOR "MEDIUM" AND "GOOD" REVERBERATION QUALITY [24]-TABLE J.1

Number of paddle positions N	$N = 100$	$N = 300$
"Medium" stirring quality	**-7.5**	**-10**
"Good" stirring quality	**-12.5**	**-15**

VI. CONCLUSION

In this paper, we presented a reverberation chamber field isotropy study for three different loading scenarios: unloaded, partially loaded, and heavily loaded chambers. In an ideal chamber, a rich isotropic environment is created no matter what type of excitation is used. Loaded-chamber isotropy deviates from the ideal case when a linearly-polarized TX antenna excites the chamber. Thus, we conclude that loading may deteriorate the field isotropy.

Loading also reduces the spatial uniformity, which then can be compensated for by applying antenna stirring. We showed that antenna stirring was not beneficial for improving the field isotropy. Other techniques need to be employed instead, such as polarization stirring or the use of polarization-balanced antennas. The approach for reducing the effects of field anisotropy demonstrated here was based on the use of the polarization-balanced antenna. It resulted in a significant reduction in the anisotropy effect.

Results obtained indicate a need for polarization stirring of the measurement antenna or for use of a polarization-balanced measurement antenna when measuring a large-form-factor DUT that cannot be rotated.

Future work on this topic is expected to involve the development of a robust test method for isotropy validation for loaded reverberation chambers. Such efforts are motivated by the fact that current test methods based on [24] do not result in the rejection of the isotropy hypothesis for a heavily loaded chamber with a vertically-polarized monopole antenna, even though obvious polarization imbalance is present.

REFERENCES

[1] D. A. Hill, *Electromagnetic Fields in Cavities*, Piscataway: Wiley IEEE Press, 2009.

[2] P.-S. Kildal, X. Chen, C. Orlenius, M. Franzen, and C. S. L. Patane, "Characterization of reverberation chambers for OTA measurements of wireles devices: Physical formulation of channel matrix and new uncertainty formula," *IEEE Trans. Antennas and Propag.*, vol. 60, no. 8, pp. 3875–3891, Aug. 2012.

[3] K. A. Remley, J. Dortmans, C. Weldon, R. D. Horansky, T. B. Meurs, C.-M. Wang, D. F. Williams, C. L. Holloway, and P. F. Wilson, "Configuring and verifying reverberation chambers for testing cellular wirelss devices," *IEEE Trans. Electromagn. Compat.*, vol. 58, no. 3, pp. 661–672, June 2016.

[4] M. Piette, “Antenna radiation efficiency measurements in a reverberation chamber,” in *Proc. Asia-Pacific Radio Science Conf.*, Aug. 24–27, 2004, pp. 19–22.

[5] H. G. Krauthauser and M. Herbrig, “Yet another antenna efficiency measurement method in reverberation chambers,” in *Proc. IEEE Int, Symp. on Electromagn. Compat.*, Jul. 25–30, 2010, pp. 536–540.

[6] C. L. Holloway, H. Shah, R. J. Pirkl, W. Young, J. Ladbury, and D. A. Hill, “Reverberation chamber techniques for determining the radiation and total efficiency of antennas,” *IEEE Trans. Antennas Propag.*, vol. 60, no. 4, pp. 1758–1770, Apr. 2012.

[7] D. Senic, D. F. Williams, K. A. Remley, C.-M. Wang, C. L. Holloway, Z. Yang, and K. F. Warnick, “Improved antenna efficiency measurement uncertainty in a reverberation chamber at millimeter-wave frequencies,” *IEEE Trans. Antennas Propag*., IN PROCESS

[8] C. L. Holloway, D. A. Hill, M. Sandroni, J. M. Ladbury, J. Coder, G. Koepke, A. C. Marwin, and Y. He, “Use of reverberation chambers to determine the shielding effectiveness of physically small, electrically large enclosures and cavities,” *IEEE Trans. Electromagn. Compat*., vol. 50, no. 4, pp. 770–782, November 2008.

[9] D. Senic, A. Sarolic, V. Roje, "GTEM cell setup and method for measuring shielding effectiveness of resonant enclosures", *International Symposium on Electromagnetic Compatibility (EMC Europe)* 2011, pp. 192 - 197.

[10] D. Senic, A. Sarolic, and Z. M. Joskiewicz, “Preliminary results of human body average absorption cross section measurements in reverberation chamber,” *International Symposium on Electromagnetic Compatibility (EMC Europe)* 2013, pp. 887-890.

[11] D. Senic, C. L. Holloway, J. M. Ladbury, G. H. Koepk, and A. Sarolic, “Absorption characteristics and SAR of a lossy sphere inside a reverberation chamber,“ *International Symposium on Electromagnetic Compatibility (EMC Europe)* 2014, pp. 962-967.

[12] I. D. Flintoft, M. P. Robinson, G. C. R. Melia, J. F. Dawson and A. C. Marvin, "Average absorption cross-section of the human body measured at 1-12 GHz in a reverberant environment: Results of a human volunteer study", *IOP Physics in Medicine and Biology*, vol. 59, no. 13, pp. 3297-3317, July 2014.

[13] I. D. Flintoft, G. C. R. Melia, M. P. Robinson, J. F. Dawson and A. C. Marvin, “Rapid and accurate broadband absorption cross-section measurement of human bodies in a reverberation chamber”, *IOP Measurement Science and Technology*, vol. 26, no. 6, pp. 065701, June 2015.

[14] D. Senic, A. Sarolic, J. M. Joskiewicz, and C. L. Holloway, "Absorption cross-section measurements of a human model in a reverberation chamber," *IEEE Trans. Electromagn. Compat*., vol. 58, no. 3, pp. 721-728, June 2016.

[15] R. J. Pirkl, K. A. Remley, and C. L. Patané, “Reverberation chamber measurement correlation,” *IEEE Trans. Electromagn. Compat.*, vol. 54, no. 3, pp. 533–545, Jun. 2012.

[16] D. Senic, K. A. Remley, C.-M. Wang, D. F. Williams, C. L. Holloway, D. C. Ribeiro, and A. T. Kirk, “Estimating and reducing uncertainty in reverberation-chamber characterization at millimeter-wave frequencies,” *IEEE Trans. Antennas and Propag.*, vol. 64, no. 7, pp. 3130–3140, Jul. 2016.

[17] P.-S. Kildal and C. Carlsson, “Detection of a polarization imbalance in reverberation chambers and how to remove it by polarization stirring when measuring antenna efficiencies,” *Microw. Opt. Technol. Lett*., vol. 34, no. 2, pp. 145–149, July 2002.

[18] R. J. Pirkl and K. A. Remley, “Experimental evaluation of the statistical isotropy of a reverberation chamber’s plane-wave spectrum,” *IEEE Trans. Electromagn. Compat.*, vol. 56, no. 3, pp. 498–509, Jun. 2014.

[19] C. Orlenius, P.-S. Kildal, and G. Poilasne, “Measurements of total isotropic sensitivity and average fading sensitivity of CDMA phones in reverberation chamber,” in *Proc. IEEE AP-S Int. Symp*., vol. 1, Washington, DC, USA, Jul. 3–8, 2005, pp. 409–412.

[20] S. J. Floris, K. A. Remley, and C. L. Holloway, “Bit error rate measurements in reverberation chambers using real-time vector receivers,” *IEEE Antennas Wireless Propag. Lett*., vol. 9, pp. 619–622, 2010.

[21] E. Genender, C. L. Holloway, K. A. Remley, J. Ladbury, and G. Koepke, “Simulating the multipath channel with a reverberation chamber: Application to bit error measurements,” *IEEE Trans. Electromagn. Compat*., vol. 52, no. 4, pp. 766–777, Nov. 2010.

[22] CTIA Certification, “Test Plan for Wireless Large-Form-Factor Device Over-the-Air Performance” Oct. 2016.

[23] J. N. H. Dortmans, K. A. Remley, D. Senic, C.-M. Wang, C. L. Holloway, “Use of absorption cross section to predict coherence bandwidth and other characteristics of a reverberation chamber setup for wireless-system tests,” *IEEE Trans. Electromagn. Compat.*, vol. 58, no. 5, pp. 1653–1661, Oct. 2016.

[24] “IEC 61000-4-21: EMC, Part 4: Testing and Measurement Techniques; Section 21: Reverberation Chamber Test Methods,” *Int. Electrotech. Comm*., Geneva, 2011.

[25] A. Al-Rawi, A. Hussain, J. Yang, M. Franzen, C. Orlenius, and A. A. Kishk, “A new compact wideband MIMO antena – The double-sided tapered self-grounded monopole array,” *IEEE Trans. Antennas and Propag.*, vol. 62, no. 6, pp. 3365–3369, Jun. 2014.